



PERGAMON

Radiation Physics and Chemistry 58 (2000) 341–356

www.elsevier.com/locate/radphyschem

**Radiation Physics
and
Chemistry**

A simplified kinetic model for the degradation of 2-butanone in aerated aqueous solutions under steady-state gamma-radiolysis

Jungsook Clara Wren*, Glenn A. Glowa

Fuel Safety Branch, Chalk River Laboratories, Chalk River, Ontario, Canada K0J 1J0

Accepted 17 November 1999

Abstract

A simplified degradation model for the continuous γ -irradiation of MEK in aerated aqueous solutions has been constructed using previously reported experimental studies and detailed kinetic model studies (Driver, P.A., Glowa, G.A., Wren, J.C., *Radiat. Phys. Chem.* 57(1), 37; Glowa, G.A., Driver, P.A., Wren, J.C., *Radiat. Phys. Chem.* 58(1), in press). The simplified model, consisting of only seven reactions and four equilibria, reproduces the experimental data and the full model results of the behaviour of MEK and the intermediate decay products and pH during the radiolysis reasonably well. The simplified model also reproduces the full model results on the dose profiles of water radiolysis products such as H^\cdot , e_{aq}^- , $^{\cdot}OH$, O_2^- and H_2O_2 very well. In this paper, the simplified model is described and the results are compared with the experimental data and simulation results from the full model. Crown Copyright © 2000 Published by Elsevier Science Ltd. All rights reserved.

Keywords: Kinetic model; Steady-state γ -radiolysis; Aqueous; 2-Butanone.

1. Introduction

We have previously reported on the experimental study and full kinetic model calculation results on the degradation of 2-butanone in aqueous solutions under steady-state γ -radiolysis (Driver et al., 2000; Glowa et al., 2000). This paper presents a simple kinetic model derived from these earlier studies.

The objective of the studies on the 2-butanone, or MEK (methyl ethyl ketone) system was to establish the impact of organic impurities on iodine chemistry in

the containment building under potential nuclear reactor accident conditions. There have been a considerable number of studies carried out on iodine behaviour under accident conditions because of the potential threat of release of radioiodine in the event of an accident. Recent reviews on iodine behaviour (Wren et al., 2000a; Wren et al., 1999 and references therein) provide comprehensive technical background on this subject. The results of these studies have established that iodine behaviour in containment could strongly depend on the pH of the containment sump, and the steady-state concentration of water radiolysis products such as $^{\cdot}OH$, O_2^- and H_2O_2 in the sump (Boyd et al., 1980; Buxton et al., 1988; Elliot, 1994; Sims, 1992; Ball et al., 1996a; Wren et al., 1992, 1996, 1999, 2000a). These studies have also shown that under containment acci-

* Corresponding author. Tel.: +1-613-584-3311; fax: +1-613-584-1220.

E-mail address: wrenc@aecl.ca (J.C. Wren).

dent conditions, organic impurities in the containment water, originating from various painted structural surfaces and other containment materials (Wren et al., 1999, 2000b), could significantly affect the pH and the concentrations of water radiolysis products (Ball et al., 1996b; Glowa, 1995; Postma and Zavadski, 1972; Wren et al., 1999). Organic iodides could also be formed by thermal and radiolytic aqueous phase reactions of I_2 with the organic impurities. The formation and decomposition of organic iodides would thus impact upon iodine volatility by changing the steady-state concentration of I_2 as well as by their own volatility.

Because of the impact of organic impurities on iodine volatility, the relative rates of the release and degradation of organic compounds, and the formation of organic iodides are very important in any model describing the time-dependent volatility of iodine following an accident. The radiolytic decomposition of organic compounds in the aqueous phase has been studied using MEK to gain a detailed mechanistic understanding from which a sound strategy for modeling the effect of organic compounds on iodine volatility in containment following an accident can be developed. MEK was chosen as a model organic compound because it is one of the common organic solvents found in paints used in containment, and because it has a relatively simple structure that simplifies the quantitative analysis of the radiolytic degradation processes.

The experimental work on the radiolytic degradation of MEK has been published previously (Driver et al., 2000). Based on these experimental results, a detailed reaction kinetic model for the steady-state γ -radiolysis of aerated aqueous solutions containing MEK was developed. The full model, consisting of about 150 reactions, reproduces the experimental data reasonably well (Glowa et al., 2000). However, the radiolytic decomposition of organic impurities is only one of the many processes or phenomena to be considered when determining iodine volatility in containment. The addition of 150 organic reactions to any containment iodine model such as LIRIC (Library of Iodine Reactions in Containment) (Wren et al., 1992, 1996, 2000c), which already contains many sets of reactions (such as water radiolysis reactions, thermal and radiolytic reactions of various iodine species, and surface reactions of iodine species), is not practical. Furthermore, MEK is only one of many organic impurities expected to influence the behaviour of iodine following an accident. Therefore, a simplified organic degradation model that is based on the mechanistic understanding gained from the full model, but is also manageable in size and can be generalized for other organic compounds, is desirable.

The degree of simplification of any kinetic model

depends on its application. Our main objective is to use the organic degradation model as a sub-set in containment iodine codes, such as LIRIC, which is used for analysis of iodine behaviour in a containment building following a postulated accident. An acceptable simplified organic model is one that will reproduce the full model results, and available experimental results, on key parameters affecting iodine behaviour. As mentioned earlier, the key parameters that need to be modelled adequately for this purpose are:

1. the pH of the containment sump, and
2. the steady state concentrations of water radiolysis products, $^{\bullet}\text{OH}$, e_{aq}^- , O_2^- and H_2O_2 in the sump (Wren et al., 1999, 2000a).

The simplified model for the radiolytic decomposition of MEK has been constructed with these objectives in mind and is the main subject of this paper. The simple model for the radiolytic degradation of MEK in aerated aqueous solutions is the first step toward obtaining a simple generic organic degradation model that can be used in iodine codes. Although it may not be necessary in terms of modelling iodine chemistry under containment accident conditions, the kinetic behaviour of the intermediate degradation products is calculated by the simple model to ensure that the simple model still includes the key mechanistic steps of the organic degradation. Prior to the presentation of the simple model, the earlier work on MEK is summarized.

2. Summary of earlier work

2.1. Experimental results on MEK decomposition

The steady-state γ -radiolysis of aqueous solutions containing $1 \times 10^{-3} \text{ mol}\cdot\text{dm}^{-3}$ MEK was studied at 25°C at a dose rate of $0.12 \text{ Gy}\cdot\text{s}^{-1}$ and adjusted to an initial pH of 10 with LiOH. The concentration used in this study was of the order of the overall organic solvent level expected to be leached into the sump from painted containment surfaces in an accident. This organic level has also been observed in both bench-scale studies and the intermediate-scale studies in the Radioiodine Test Facility (Wren et al., 1999). Experiments using MEK were conducted in air-, argon- or nitrous oxide-purged aqueous solutions, or in argon-purged solutions with *t*-butanol added. However, the main focus was on the air-purged system. The concentrations of MEK and some of its radiolytic products were analyzed as a function of time. The change in pH as a result of the MEK decomposition was also measured as a function of time.

The *G*-values for the initial loss of MEK and the pseudo-first order rate constants for the MEK de-

Table 1
Initial G -value of MEK degradation under various conditions

Condition	Dominant specie(s) present	Initial G -value
Argon purged, 0.5 M <i>t</i> -butanol	$e_{(aq)}^-$	1.4
Argon purged	$e_{(aq)}^-$ and $\cdot\text{OH}$	2.8
Aerated	$e_{(aq)}^-$, $\cdot\text{OH}$ and O_2	2.9
N_2O purged	$\cdot\text{OH}$ (G -value = 5.3)	5.6

composition observed under various conditions are shown in Table 1 and Fig. 1, respectively. Under de-aerated conditions, the G -value and the first-order rate constant observed in the N_2O purged solution are about twice those observed in the argon-purged solution. This is consistent with the assumption that the initial step is mainly hydrogen abstraction from MEK by $\cdot\text{OH}$ to form the MEK radical, MEK^\cdot . When $\cdot\text{OH}$ was removed from the aqueous solutions as in the case of *t*-butanol solutions, MEK was found to decay at a reduced rate. The initial G -value for the loss of MEK observed in the aerated solution also reflects the G -value of $\cdot\text{OH}$ production in aerated solutions.

However, the overall first-order rate of MEK decay appears to be affected by the presence of oxygen as well as by the $\cdot\text{OH}$ production rate. The first order rate constant observed in the aerated solution is almost twice that of the argon purged solution even though the G -value for the initial loss of MEK is about the same for both cases. In aerated solutions, MEK^\cdot reacts with O_2 to form MEK peroxy radical, which further reacts and eventually produces a significant amount of smaller oxidized species (further discussion below). In de-aerated solutions, the main decay path of MEK^\cdot is

considered to be dimerization, forming compounds such as 3,4 dimethyl 2,5 hexanedione, which decomposes to reform MEK.

In the presence of oxygen, MEK $^\cdot$ reacts primarily with oxygen to form the MEK peroxy radical (MEK- O_2^\cdot). This peroxy radical can dimerize to form a tetroxide intermediate, which decomposes to form the observed intermediate products, 3-hydroxy-2-butanone, 2,3-butanedione, and acetaldehyde. The concentrations of these products were measured as a function of time, except for 2,3-butanedione, because of problems associated with its derivatization prior to HPLC analysis. The formation of organic acids, and eventually CO_2 , reduces the pH of the solutions. The pH change as a function of dose was also measured. The experimental results are shown in the following sections in comparison with the model simulation results.

2.2. Summary of full model

Based on the experimental and literature data, a comprehensive reaction kinetic model for the radiolytic decomposition of MEK in aerated aqueous solutions

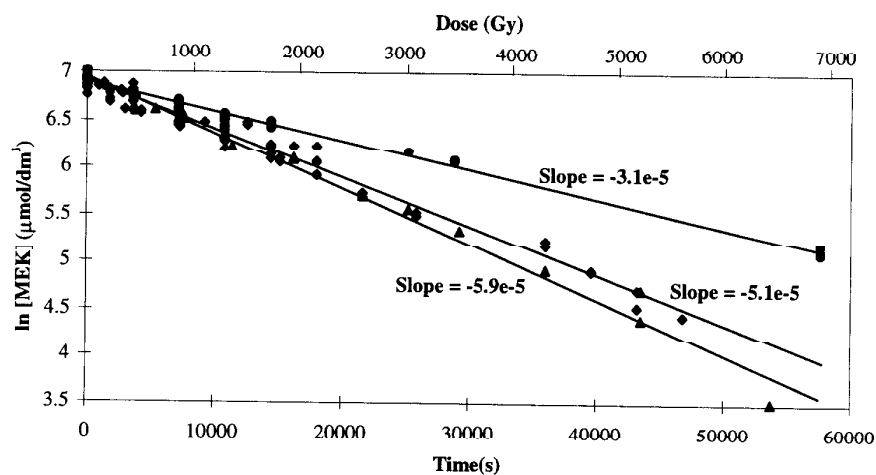


Fig. 1. Pseudo-first order plots of MEK decomposition observed in aerated (\blacklozenge), argon-purged (\bullet) and nitrous oxide-purged (\blacktriangle) solutions.

was developed. The reactions included in the full kinetic model, with the literature sources of the rate constants, have been presented previously (Glowa et al., 2000). The full model contains about 130 reactions involving MEK and its decomposition products, in addition to about 25 water radiolysis reactions. The proposed MEK decay path included in the full model is briefly described below.

The first step for the decomposition of MEK in aerated aqueous solutions is the reactions with a water radiolysis product such as $\cdot\text{OH}$, $\cdot\text{H}$ and e_{aq}^- . The behaviour of the reactive water radiolysis products is thus included in modelling the MEK decomposition. The main route for the first decomposition step is the abstraction of hydrogen by $\cdot\text{OH}$ to form the MEK radical. The MEK radical either reacts with O_2 or undergoes dimerization/disproportionation reactions. In aerated solutions, however, the radical decays mainly by its reaction with O_2 to form an organic peroxy radical.

The MEK peroxy radical undergoes dimerization to form a tetroxide compound, which can then break down into various products including 3-hydroxy-2-butanone ($\text{CH}_3\text{COCH}(\text{OH})\text{CH}_3$), 2,3-butanedione ($\text{CH}_3\text{COCOCH}_3$), and acetaldehyde (CH_3CHO). These intermediate decomposition products, 3-hydroxy-2-butanone, 2,3-butanedione and acetaldehyde, are subject to similar radiolytic decay paths as MEK, (i.e., abstraction of hydrogen atoms by hydroxyl radicals, followed by the reaction with dissolved oxygen, etc.), to form acetaldehyde, acetic acid, formaldehyde and formic acid. These products further decompose radiolytically to CO_2 . Acid–base equilibria associated with acidic decay products such as acetic acid, formic acid,

and dissolved CO_2 ($\text{H}_2\text{CO}_3/\text{HCO}_3^-/\text{CO}_3^{2-}$), are also included in the model.

The full model simulation results for MEK and the decomposition products are in reasonable agreement with the experimental data. The full model simulation results have been previously presented (Glowa et al., 2000) and are compared in the present work with the simplified model simulation results.

3. Simplified model

The simplified model developed for the radiolytic degradation of MEK in aerated aqueous solutions consists of seven radiolytic reactions, the acetic acid equilibrium and the CO_2 /carbonate equilibria (Table 2). The construction of the simplified model was possible because:

1. The kinetic behaviour of the water radiolysis products that are the key reactants for the organic degradation, could be treated in a relatively simple way (i.e., near steady-state) during continuous γ -radiolysis of aqueous solutions,
2. The rate determining step from one molecular species to the next molecular species in the degradation series is hydrogen abstraction by $\cdot\text{OH}$ (or e_{aq}^- attachment in the case of diones). That is, subsequent reactions leading to the next molecular product (i.e., organic peroxide formation and decomposition) can be ignored, and
3. The steady-state approximation was applicable for many intermediate steps.

These assumptions and the kinetic analyses that were

Table 2
Reactions in the simplified model

	Reaction ^a	Rate constant ^b
R1	$\text{MEK} + \cdot\text{OH} \rightarrow 3\text{-Hydroxy-2-butanone (or IP1)}$	$(0.25)(7.3 \times 10^8)$
R2	$\text{MEK} + \cdot\text{OH} \rightarrow 2,3\text{-Butanedione (or IP2)}$	$(0.75)(7.3 \times 10^8)$
R3	$3\text{-Hydroxy-2-butanone} + \cdot\text{OH} \rightarrow \text{Acetic acid} + \text{Acetaldehyde}$	1.2×10^9
R4	$2,3\text{-Butanedione} + \cdot\text{OH} \rightarrow \text{Acetic acid} + \text{Acetaldehyde}$	1.7×10^8
R5	$2,3\text{-Butanedione} + e_{\text{aq}}^- \rightarrow \text{Acetic acid} + \text{Acetaldehyde}$	1.0×10^{10}
R6	$\text{Acetaldehyde} + \cdot\text{OH} \rightarrow 2\text{CO}_2$	3.6×10^9
R7	$\text{Acetic acid} + \cdot\text{OH} \rightarrow 2\text{CO}_2$	$1 \times 10^8 \cdot (1 + K_{\text{aq}}/[\text{H}^+])^c$
E1	$\text{Acetic acid} \leftrightarrow \text{H}^+ + \text{Acetate (pK}_a = 4.75)$	$k_f = 1.78 \times 10^5, k_b = 1 \times 10^{10}$
E2	$\text{H}_2\text{O} + \text{CO}_2 \leftrightarrow \text{H}_2\text{CO}_3$	$k_f = 0.3, k_b = 20$
E3	$\text{H}_2\text{CO}_3 \leftrightarrow \text{H}^+ + \text{HCO}_3^- (\text{pK}_a = 6.3)$	$k_f = 2 \times 10^6, k_b = 1 \times 10^{10}$
E4	$\text{HCO}_3^- \leftrightarrow \text{H}^+ + \text{CO}_3^{2-} (\text{pK}_a = 10.25)$	$k_f = 0.484, k_b = 1 \times 10^{10}$

^a Note: Equations are balanced in terms of carbon content only.

^b For equilibria, k_f and k_b represent the forward and backward rate constants, respectively. The forward rate constants, k_f , for E1, E3 and E4 are first order rate constants in units of s^{-1} . All the other rate constants are second order rate constants in units of $\text{dm}^3 \cdot \text{mol}^{-1} \cdot \text{s}^{-1}$.

^c K_{aq} is k_f/k_b of Equilibrium E1.

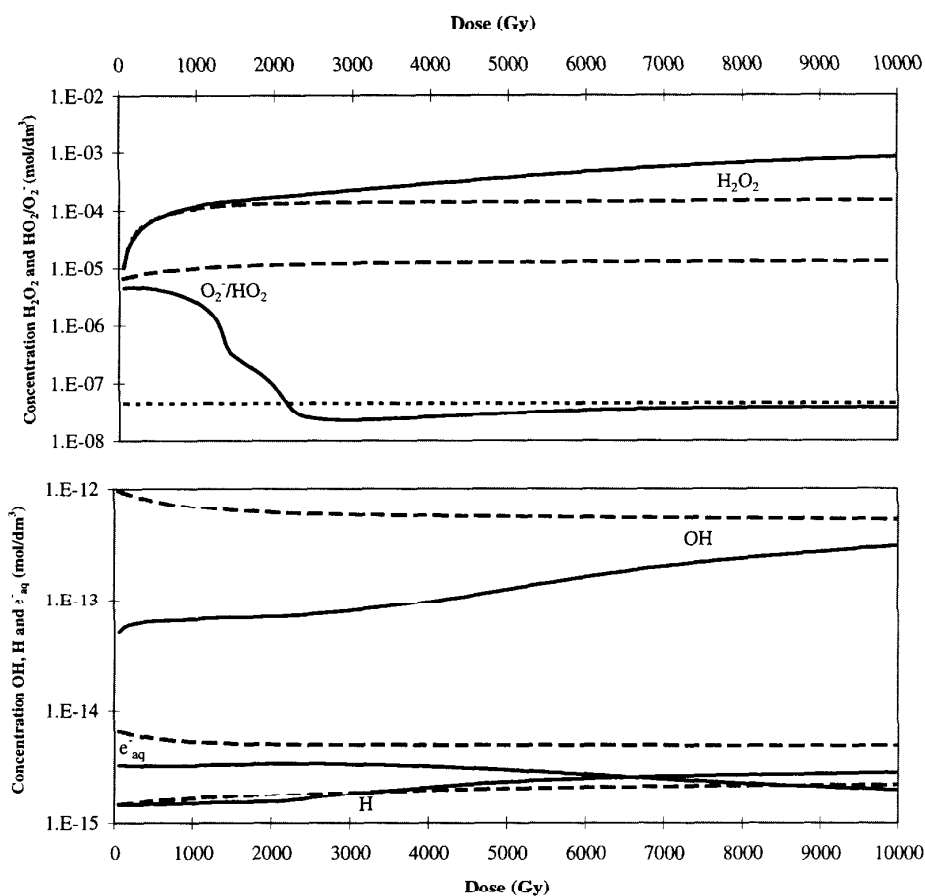


Fig. 2. Concentrations of water radiolysis products calculated by the full model in the presence and absence of MEK: Solid line (with MEK), Dashed line (No MEK, pH 10). Dotted line is O_2^-/HO_2 (No MEK, pH 4.3).

used to construct the simplified model from the full model, and the model simulation results are discussed in detail in the following sections.

The simplified model simulation results shown in this paper were calculated using the numerical integration solver FACSIMILE¹ for all the reactions presented in Table 2, coupled with water radiolysis reactions.

¹ The FACSIMILE program is a commercial integration package (AEA Technologies, Harwell Laboratory, Oxfordshire, UK) for solving coupled-differential equations which was specifically designed for chemical systems. The chemical system to be modelled is expressed as a series of simple chemical reactions, which is then converted into coupled differential equations and solved by FACSIMILE's numerical integration method.

3.1. Behaviour of water radiolysis products

The radiolytic degradation of MEK in aqueous solutions occurs via reactions with water radiolysis products. Understanding the kinetic behaviour of these water radiolysis products are thus important in the development of a simplified organic degradation model. Fig. 2 shows the concentrations of water radiolysis products in aerated water in the presence and absence (i.e., pure aerated water) of MEK during continuous γ -radiolysis, as calculated by the full model. These results show some of the key conditions which lead to the development of a simple model.

1. The concentrations of $\cdot OH$, H , e_{aq}^- change slowly with time (or total absorbed dose) during continuous γ -radiolysis. These near steady-state conditions simplify the analysis of the full model results which,

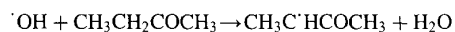
- consequently, enables the development of the simplified model.
- The concentrations of H^\cdot and e_{aq}^- are 2–3 orders of magnitude lower than that of $\cdot\text{OH}$ in aerated aqueous solutions, where the main decay path of the electrons produced by water radiolysis is the reaction with dissolved oxygen, which is assumed to remain saturated due to interfacial mass transfer. Hence, unless their specific reactivities (or the rate constants) are about 1–2 orders of magnitude higher than that of $\cdot\text{OH}$, the decay path of MEK via reactions with H^\cdot or e_{aq}^- can be ignored (see further discussion later).
 - The differences in the H^\cdot and e_{aq}^- concentrations in the absence of MEK and in the presence of MEK are relatively small, compared to the case of $\cdot\text{OH}$. The differences in the H^\cdot and e_{aq}^- concentrations are also partly due to the change in pH during MEK degradation, rather than their direct involvement in the reactions with MEK, because the pseudo-steady-state concentrations of water radiolysis products of pure water are pH dependent. The difference in the $\cdot\text{OH}$ concentration is, however, significantly more than expected as a result of pH change. This indicates that the main degradation of MEK is via reactions with $\cdot\text{OH}$ (see further discussion below). Note that the results calculated for pure oxygenated water shown in Fig. 2 are those at a constant pH 10. The calculations for pure oxygenated water were also performed at lower pH values, but the results are not shown in the figure (except for HO_2/O_2^-) for clarity.
 - The difference in the sum of the HO_2 and O_2^- concentrations ($\text{HO}_2 \leftrightarrow \text{H}^+ + \text{O}_2^-$, $\text{pK}_a = 4.8$) calculated in the presence and absence of MEK is due to the change in pH, not as a result of their direct involvement in the MEK degradation reactions. The HO_2/O_2^- concentration in the presence of MEK approaches the calculated value in the absence of MEK at pH 4.3, as the pH of the irradiated MEK solution approaches that value (Fig. 2).
 - The difference observed for H_2O_2 is also mainly induced by the changes in the $\cdot\text{OH}$ and e_{aq}^- concentrations during the MEK degradation, not as a result of its direct involvement in the MEK reactions. For a given dose rate, the concentration of H_2O_2 during continuous γ -radiolysis of water is determined mainly by the primary production rate (i.e., G -value of H_2O_2) and its decomposition rates by reactions with $\cdot\text{OH}$ and e_{aq}^- . The reduction in the $\cdot\text{OH}$ and e_{aq}^- concentrations due to their reactions with MEK results in an increase in the pseudo-steady-state concentration of H_2O_2 .

The relative importance of $\cdot\text{OH}$ reactions versus those of H^\cdot and e_{aq}^- in the MEK decay can be rationalized

further by examining the rates (i.e., concentration \times rate constant) of their reactions with MEK and its intermediate molecular products. It is shown in Fig. 2 that during the MEK degradation the concentrations of H^\cdot and e_{aq}^- are about 2–3 orders of magnitude lower than that of $\cdot\text{OH}$. In general, the rate constant for hydrogen abstraction from an organic compound by H^\cdot is about an order of magnitude lower than that of $\cdot\text{OH}$. Thus, the decay path of MEK via reactions with H^\cdot is negligible compared to those with $\cdot\text{OH}$. The rate constant of e_{aq}^- reaction with an organic compound containing a carbonyl group is generally larger than that of $\cdot\text{OH}$. However, because of the lower concentration, the rate constant of e_{aq}^- reaction of a given organic species should be about two orders of magnitude larger than that of $\cdot\text{OH}$, in order for the decay path of an organic compound by the electron reactions to become important (as in 2,3-butanedione case, discussion in Section 3.4). Thus, the reactions of MEK and its intermediate degradation products with H^\cdot and e_{aq}^- were ignored in constructing the simplified model, except for the reaction of 2,3-butanedione with e_{aq}^- .

3.2. Initial MEK decay reactions

The MEK concentration shows an exponential decrease with increasing radiation dose, indicating a pseudo-first order decomposition of MEK under the steady-state γ -radiolysis conditions (Figs. 1 and 3). This is because the initiation of the MEK decay is mainly by reaction with $\cdot\text{OH}$, a water radiolysis product which has reached a constant concentration under these conditions.



$$k_1 = 7.3 \times 10^8 \text{ dm}^3 \cdot \text{mol}^{-1} \cdot \text{s}^{-1} \text{ (Mezyk, 1994)} \quad (1)$$

The reactions of MEK with H^\cdot and e_{aq}^- are less important because of the reasons described above, and were ignored in constructing the simplified model. The simplified model reproduces the full model MEK decay curve as well as the experimental data (Fig. 3). The small difference observed between the full model and the simplified model calculations is considered to be due to the omission of the reactions of MEK with H^\cdot and e_{aq}^- .

It should be noted that the behaviour of hydroxyl radicals formed by water radiolysis is important to MEK decay kinetics, as well as when determining iodine behaviour in the containment sump (Driver et al., 2000, Wren et al., 1999, 2000a). Any model describing the effects of organic impurities on iodine volatility in an accident must describe the behaviour of the $\cdot\text{OH}$ radical. The behaviour of $\cdot\text{OH}$ is also modelled by the simplified model given in Table 2 and the results are

discussed later in Section 3.6. However, some analysis of the behaviour of $\cdot\text{OH}$ during the MEK degradation is given below, which provides better understanding of the radiolytic degradation process.

The MEK decay in aerated solutions, and also in nitrous oxide and argon-purged solutions, was observed to follow first-order kinetics (Fig. 1). These linear plots of $\ln [\text{MEK}]$ versus dose (or time at a constant dose rate) also indicate that the $\cdot\text{OH}$ concentration is at, or near, steady-state during the decomposition of MEK, because

$$\frac{d[\text{MEK}]}{dt} = k_1 \cdot [\cdot\text{OH}] \cdot [\text{MEK}]. \quad (2)$$

If the $\cdot\text{OH}$ concentration is constant with time, i.e., at a steady-state, the rate law results in

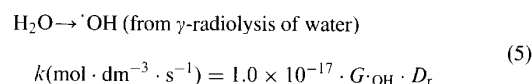
$$[\text{MEK}]_t = [\text{MEK}]_0 \cdot \exp(-k_1 \cdot [\cdot\text{OH}]_{\text{ss}} \cdot t) \quad (3)$$

$$\text{or } [\text{MEK}]_t = [\text{MEK}]_0 \cdot \exp\left(-k_1 \cdot [\cdot\text{OH}]_{\text{ss}} \cdot \left(\frac{D_t}{D_r}\right)\right), \quad (4)$$

where the reaction time, t (in units of s), the total absorbed dose at time t , D_t (in units of Gy) and the dose rate, D_r (in units of $\text{Gy}\cdot\text{s}^{-1}$). Thus, the concentration of MEK decreases exponentially and the slope of the plot of $\ln [\text{MEK}]$ versus time (or total absorbed dose) is determined by $-k_1 \cdot [\cdot\text{OH}]_{\text{ss}}$ (or $(-k_1/D_r) \cdot [\cdot\text{OH}]_{\text{ss}}$).

The primary production of $\cdot\text{OH}$ from water radiolysis and its subsequent reactions with other water radiolysis products, as well as with MEK and other species present in water (e.g., MEK decay products), should be considered in determining the concentration of the

$\cdot\text{OH}$ radical. However, at the MEK concentration used in the test ($1 \times 10^{-3} \text{ mol}\cdot\text{dm}^{-3}$), $\cdot\text{OH}$ decays primarily by the reaction with MEK and its decay products. Furthermore, the reaction rate constants of the decay products with $\cdot\text{OH}$ are similar to that of MEK, in the range of 0.7×10^9 [for MEK (Mezyk, 1994)] to $3.6 \times 10^9 \text{ dm}^3 \text{ mol}^{-1}\cdot\text{s}^{-1}$ [for acetaldehyde (Schuchmann and von Sonntag, 1988)]. Thus, the behaviour of $\cdot\text{OH}$ can be approximated by the following two simplified reactions:



The rate of radiolytic formation of $\cdot\text{OH}$ (Reaction 5) is $1.0 \times 10^{-7} \cdot G_{\cdot\text{OH}} \cdot D_r$ (units of $\text{mol}\cdot\text{dm}^{-3}\cdot\text{s}^{-1}$) where $G_{\cdot\text{OH}}$ is the G -value for the $\cdot\text{OH}$ production from water radiolysis in units of number of molecules produced per 100 eV absorbed dose, D_r is the absorbed dose rate in units of $\text{Gy}\cdot\text{s}^{-1}$. RH in Reaction (6) represents either MEK or a hydrogen-containing decomposition product.

Under these conditions, one can approximate the steady-state concentration of $\cdot\text{OH}$ by assuming that during the MEK decomposition, the total organic concentration, $[\Sigma\text{RH}]$, is constant at the initial MEK concentration level;

$$[\Sigma\text{RH}]_t \approx [\text{MEK}]_0 \quad (7)$$

and the rate constant of the reaction of these decomposition products with $\cdot\text{OH}$ is the same as that of MEK ($7.3 \times 10^8 \text{ dm}^3\cdot\text{mol}^{-1}\cdot\text{s}^{-1}$). The steady-state con-

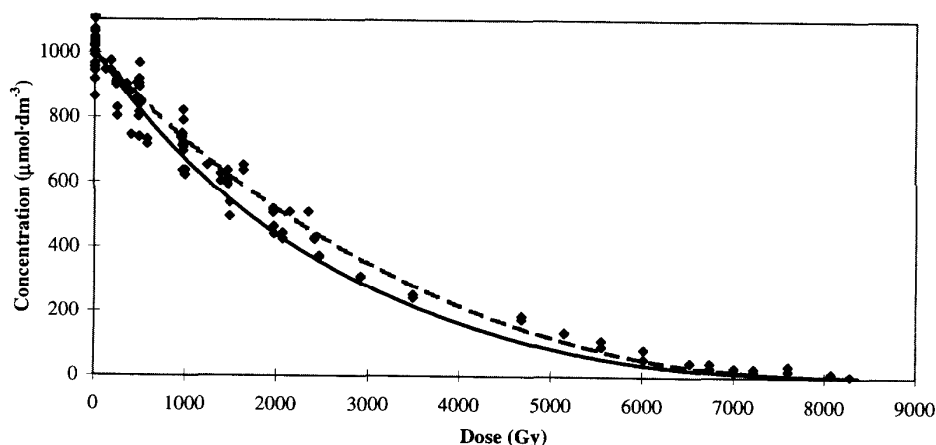


Fig. 3. Dose profile of MEK: experimental data (\blacklozenge), full model prediction (—), and simplified model prediction (---).

centration of $\cdot\text{OH}$ is then

$$\frac{d[\cdot\text{OH}]_{\text{ss}}}{dt} \approx 1 \times 10^{-7} \cdot G_{\cdot\text{OH}} \cdot D_r - 7.3 \times 10^8 \cdot [\cdot\text{OH}]_{\text{ss}} \cdot [\Sigma\text{RH}]_t \approx 0, \text{ and} \quad (8)$$

$$[\cdot\text{OH}]_{\text{ss}} \approx \frac{1 \times 10^{-7} \cdot G_{\cdot\text{OH}} \cdot D_r}{7.3 \times 10^8 \cdot [\Sigma\text{RH}]_t} \approx \frac{1 \times 10^{-7} \cdot G_{\cdot\text{OH}} \cdot D_r}{7.3 \times 10^8 \cdot [\text{MEK}]_0}, \quad (9)$$

yielding the steady-state $\cdot\text{OH}$ concentration of $4.5 \times 10^{-14} \text{ mol}\cdot\text{dm}^{-3}$ using a $G_{\cdot\text{OH}}$ value of 2.7 molecules per 100 eV absorbed dose, a D_r value of $0.12 \text{ Gy}\cdot\text{s}^{-1}$ and $[\text{MEK}]_0$ of $1 \times 10^{-5} \text{ mol}\cdot\text{dm}^{-3}$. Note that Equation (9) states the steady-state $\cdot\text{OH}$ concentration is proportional to dose rate.

The $\cdot\text{OH}$ concentration calculated using the full MEK reaction model, shown in Fig. 2, varies slightly with the total absorbed dose (or time) up to 5000 Gy at which point 90% of MEK has decomposed. (The $\cdot\text{OH}$ concentration calculated using the simplified MEK model is discussed in Section 3.6). Note that the presence of about $1 \times 10^{-3} \text{ mol}\cdot\text{dm}^{-3}$ organic impurities considerably lowers the steady-state $\cdot\text{OH}$ concentration. The analytically obtained $\cdot\text{OH}$ concentration, $4.5 \times 10^{-14} \text{ mol}\cdot\text{dm}^{-3}$, is close to the full model value, $5\text{--}6 \times 10^{-14} \text{ mol}\cdot\text{dm}^{-3}$, at doses less than 5000 Gy, indicating that the gross approximations for the $\cdot\text{OH}$ production and decomposition [Reactions (5) to (7)] may be used, if the reduction of water radiolysis reactions is desirable.

If the organic level is low, such that it does not completely dictate the $\cdot\text{OH}$ concentration (less than $1 \times 10^{-4} \text{ mol}\cdot\text{dm}^{-3}$), the reactions of water radiolysis products with $\cdot\text{OH}$ should be considered in determining the steady-state concentration of $\cdot\text{OH}$ (Driver et al., 2000). Likewise, if the I^- concentration is high, as is expected under reactor accident conditions, the reaction between I^- with $\cdot\text{OH}$ should also be considered. It should be noted that, for a given dose rate, the reduction of $\cdot\text{OH}$ concentration as a result of the reaction with organic compounds also increases the concentration of H_2O_2 , which is a key iodine reductant in the event of an accident.

The steady-state assumption for $\cdot\text{OH}$ concentration and its analytically derived steady-state concentration were also examined by comparing the observed slope of the first-order MEK decay plot and the calculated slope from Eq. (3). The slope of the plot for the aerated solution in Fig. 1 is $5.1 \times 10^{-5} \text{ s}^{-1}$. The analytically derived value using Eqs. (3) and (9) is $-3.3 \times 10^{-5} \text{ s}^{-1}$, somewhat lower than the observed slope. The main reason for the discrepancy is that the analytical solution yields a lower $\cdot\text{OH}$ concentration.

Using an average $\cdot\text{OH}$ concentration of $6 \times 10^{-14} \text{ mol}\cdot\text{dm}^{-3}$, as calculated from the full model, Eq. (3) yields a slope of $-4.4 \times 10^{-5} \text{ s}^{-1}$, supporting the assumption that the $\cdot\text{OH}$ reactions with MEK and the intermediate molecular products are the main MEK decay mechanism.

3.3. Formation of 3-hydroxy-2-butanone and 2,3-butanedione

The initial MEK reaction produces the MEK radical, $\text{MEK}\cdot$, which in aerated solutions reacts rapidly with O_2 :



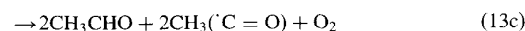
where $\text{MEK}\cdot$ represents one of the three possible hydrogen abstraction products: $\text{CH}_3(\cdot\text{CH})\text{COCH}_3$, $(\cdot\text{CH}_2)\text{CH}_2\text{COCH}_3$, and $\text{CH}_3\text{CH}_2\text{CO}(\cdot\text{CH}_2)$. The MEK radical is expected to be at a pseudo steady-state, with the pseudo-steady-state concentration being

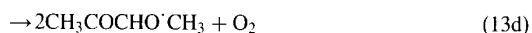
$$\frac{d[\text{MEK}\cdot]_t}{dt} = k_1 \cdot [\cdot\text{OH}]_{\text{ss}} \cdot [\text{MEK}]_t - k_{10} \cdot [\text{MEK}\cdot]_t \cdot [\text{O}_2] \approx 0. \quad (11)$$

$$[\text{MEK}\cdot]_t = \frac{k_1 \cdot [\cdot\text{OH}]_{\text{ss}} \cdot [\text{MEK}]_t}{k_{10} \cdot [\text{O}_2]_0}. \quad (12)$$

Because $[\text{MEK}]$ changes with time (see Eq. 3), $[\text{MEK}\cdot]_t$ is not at a true steady-state but changes slowly with time. (Owing to the fact that $[\text{MEK}]$ changes very slowly, it can be treated as a constant over the integration time interval. Therefore, the steady-state approximation used in Eq. (11) is still valid, and the relationship given in Eq. (12) still applies to $[\text{MEK}\cdot]_t$ as a function of time.) The dissolved oxygen concentration is assumed to be saturated and constant with time in the experiments because of efficient gas-aqueous interfacial mass transfer of oxygen relative to the degradation rate.

By analogy to the acetone system studied by Zegota et al. (1986), the MEK peroxy radical, $\text{MEKO}_2\cdot$ or $\text{CH}_3\text{CH}(\text{O}_2\cdot)\text{COCH}_3$, is assumed to dimerize to form a tetroxide compound, which then decomposes rapidly to 3-hydroxy-2-butanone ($\text{CH}_3\text{CH}(\text{OH})\text{COCH}_3$), 2,3-butanedione ($\text{CH}_3\text{COCOCH}_3$), and acetaldehyde (CH_3CHO):





The initial formation rates of the intermediate products, 3-hydroxy-2-butanone (IP1), 2,3-butanedione (IP2) and acetaldehyde (IP3), are then determined by the following rate law;

$$\frac{d[\text{IP}_x]}{dt} = f_{\text{IP}_x} \cdot k_{\text{TI}} \cdot [\text{MEKO}_2]_{\text{ss}}^2 \quad (14)$$

where IP_x represents the intermediate product (IP1, IP2 or IP3), f_{IP_x} represents the branching fraction for the intermediate, IP_x (detailed definition of f_{IP_x} is discussed later). The overall decay rate constant of the tetroxide intermediate, k_{TI} ($=k_{13a} + k_{13b} + k_{13c} + k_{13d}$) is estimated to be $8 \times 10^8 \text{ dm}^3 \cdot \text{mol}^{-1} \cdot \text{s}^{-1}$ based on the acetone system as described in the full model (Glowa et al., 2000).

Assuming a pseudo steady-state also for MEK peroxy radical, its concentration is determined as follows:

$$\frac{d[\text{MEKO}_2]}{dt} = k_{10} \cdot [\text{MEK}'] \cdot [\text{O}_2] - k_{\text{TI}} \cdot [\text{MEKO}_2]^2 \approx 0. \quad (15)$$

By substituting $[\text{MEK}']_t$ from Eq. (12), for $[\text{MEK}']$

$$k_{\text{TI}} \cdot [\text{MEKO}_2]_t^2 \approx k_{10} \cdot [\text{MEK}']_t \cdot [\text{O}_2]_0 \approx k_1 \cdot [\text{OH}]_{\text{ss}} \cdot [\text{MEK}]_t \quad (16)$$

The rate equation for intermediate product, IP_x, is thus [using Eq. (3)]

$$\frac{d[\text{IP}_x]}{dt} \approx f_{\text{IP}_x} \cdot k_1 \cdot [\text{OH}]_{\text{ss}} \cdot [\text{MEK}]_t \approx f_{\text{IP}_x} \cdot k_1 \cdot [\text{OH}]_{\text{ss}} \cdot [\text{MEK}]_0 \cdot \exp(-k_1 \cdot [\text{OH}]_{\text{ss}} \cdot t) \quad (17)$$

resulting in

$$[\text{IP}_x]_t \approx f_{\text{IP}_x} \cdot [\text{MEK}]_0 \cdot (1 - \exp(-k_1 \cdot [\text{OH}]_{\text{ss}} \cdot t)) \quad (18)$$

since $[\text{IP}_x] = 0$ at time 0.

For small t ($t \ll \frac{1}{k_1 \cdot [\text{OH}]_{\text{ss}}} \approx 10^5 \text{ s}$), the rate equation further simplified to

$$[\text{IP}_x]_t \approx f_{\text{IP}_x} \cdot k_1 \cdot [\text{OH}]_{\text{ss}} \cdot [\text{MEK}]_0 \cdot t \quad (19)$$

$$\text{or } [\text{IP}_x]_t \approx f_{\text{IP}_x} \cdot k_1 \cdot [\text{OH}]_{\text{ss}} \cdot [\text{MEK}]_0 \cdot \left(\frac{D_t}{D_t} \right). \quad (20)$$

The branching fractions, f_{IP_x} , for the production of these intermediate species is

$$f_{\text{IP1}} = (1/2k_{13b} + k_{13d}) / (k_{13a} + k_{13b} + k_{13c} + k_{13d}) = 0.22 \text{ for 3-hydroxy-2-butanone,}$$

$$f_{\text{IP2}} = (k_{13a} + 1/2k_{13b}) / (k_{13a} + k_{13b} + k_{13c} + k_{13d}) = 0.72 \text{ for 2,3-butanedione and}$$

$$f_{\text{IP3}} = k_{13c} / (k_{13a} + k_{13b} + k_{13c} + k_{13d}) = 0.06 \text{ for acetaldehyde,}$$

based on the rate constants of Reactions (13a)–(13d) used in the full model. These branching fractions thus yield the following calculated initial slopes of each concentration versus total absorbed dose plots:

$$\begin{aligned} &5.9 \times 10^{-8} \text{ mol} \cdot \text{dm}^{-3} \cdot \text{Gy}^{-1} \quad (\text{or } 0.57 \text{ molecules} \cdot (100 \text{ eV})^{-1}) \text{ for 3-hydroxy-2-butanone,} \\ &1.9 \times 10^{-7} \text{ mol} \cdot \text{dm}^{-3} \cdot \text{Gy}^{-1} \quad (\text{or } 1.9 \text{ molecules} \cdot (100 \text{ eV})^{-1}) \text{ for 2,3-butanedione, and} \\ &1.6 \times 10^{-8} \text{ mol} \cdot \text{dm}^{-3} \cdot \text{Gy}^{-1} \quad (\text{or } 0.16 \text{ molecules} \cdot (100 \text{ eV})^{-1}) \text{ for acetaldehyde.} \end{aligned}$$

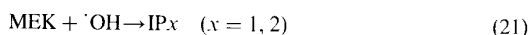
The initial slope corresponds to the *G*-value of the process which can also be expressed in molecules·(100 eV)⁻¹. The initial slope calculated for 3 hydroxy 2 butanone is close to the experimentally observed slope, $(5 \pm 1) \times 10^{-8} \text{ mol} \cdot \text{dm}^{-3} \cdot \text{Gy}^{-1}$ (Fig. 4). Note that the dose profile of 2,3-butanedione was not obtained experimentally owing to the problems associated with the HPLC analysis (Driver et al., 2000). The calculated dose profiles of 2,3-butanedione are shown in Fig. 5.

For acetaldehyde, the slope was observed to be about $(3 \pm 1) \times 10^{-8} \text{ mol} \cdot \text{dm}^{-3} \cdot \text{Gy}^{-1}$ (Fig. 6), larger than the calculated value. This discrepancy is likely caused by fact that acetaldehyde is mainly formed from the intermediate products, 3-hydroxy-2-butanone and 2,3-butanedione (see discussion below). In fact, the direct formation of acetaldehyde from the MEK tetroxide intermediate can be ignored in approximating the behaviour of acetaldehyde. Therefore, in constructing the simplified model Reaction (13c) is ignored and the branching fractions for 3-hydroxy-2-butanone and 2,3-butanedione are taken to be 0.25 and 0.75, respectively.

If there is no decomposition of IP_x, its concentration would reach a maximum value of $f_{\text{IP}_x} \cdot [\text{MEK}]_0$ [see Eq. (18)]. However, IP_x does decompose in the presence of radiation, resulting in the concentration decrease observed at longer times. It should be noted that the above analysis uses a steady-state approximation for $\cdot\text{OH}$ concentration for simplicity, but the $\cdot\text{OH}$ concentration is calculated as a function of time in the simplified model by the coupled differential equations solver (FACSIMILE).

3.4. Decomposition of 3-hydroxy-2-butanone and 2,3-butanedione to acetaldehyde and acetic acid

The analysis above indicates that the various steps between Reactions (1) and (13) in the full model can be reduced to



with a rate constant, $f_{\text{IP}_x} \cdot k_1$, where IP_x is 3 hydroxy 2

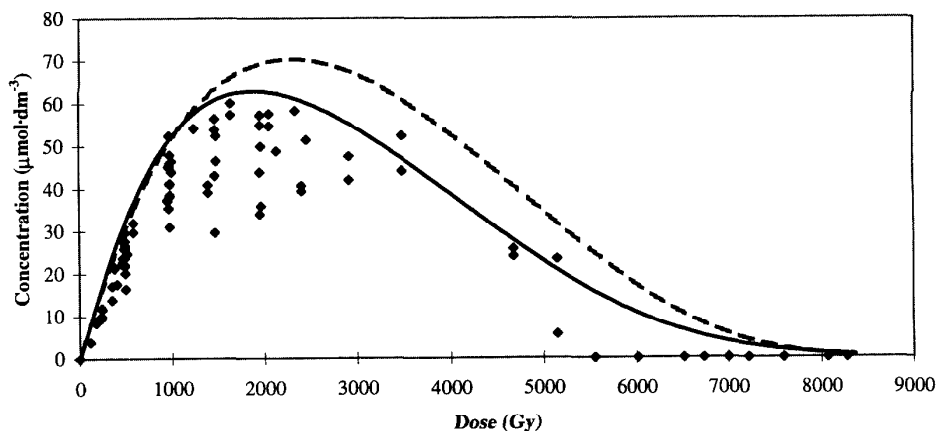
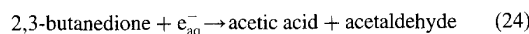
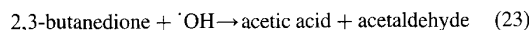
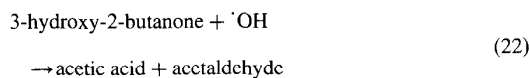


Fig. 4. Dose profile of 3-hydroxy-2-butanone: experimental data (◆), full model prediction (—), and simplified model prediction (---).

butanone ($x = 1$) or 2,3-butanedione ($x = 2$). That is, subsequent reactions, leading to IP x formation following the initial hydrogen abstraction from MEK by $\cdot\text{OH}$, are ignored.

These intermediate products further decompose to acetaldehyde and acetic acid. The concentrations of acetaldehyde and acetic acid were measured as a function of dose (or time) (Figs. 6 and 7, respectively). Thus, not only the dose profile of 3-hydroxy-2-butanone, but also the dose profiles of acetic acid and acetaldehyde were analyzed to determine the key decomposition steps for 3-hydroxy-2-butanone (IP1) and 2,3-butanedione (IP2). In the simplified model these decomposition steps are reduced to



The decomposition mechanisms of IP1 and IP2 to acetic acid and acetaldehyde are considered to be similar to the decomposition of MEK and, thus, can be simplified to one reaction step as shown in Reactions (22)–(24). For the decomposition of 3-hydroxy-2-butanone, the hydrogen abstraction by $\cdot\text{OH}$ (Reaction 25)

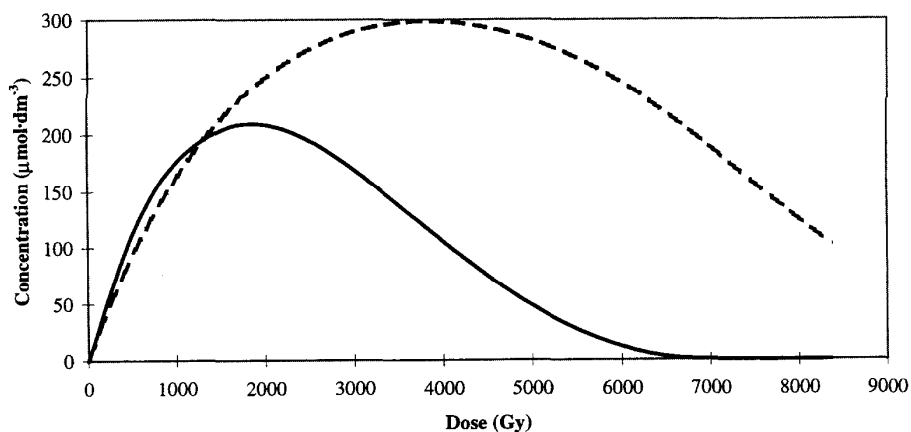


Fig. 5. Calculated dose profile of 2,3-butanedione: full model prediction (—), and simplified model prediction (---).

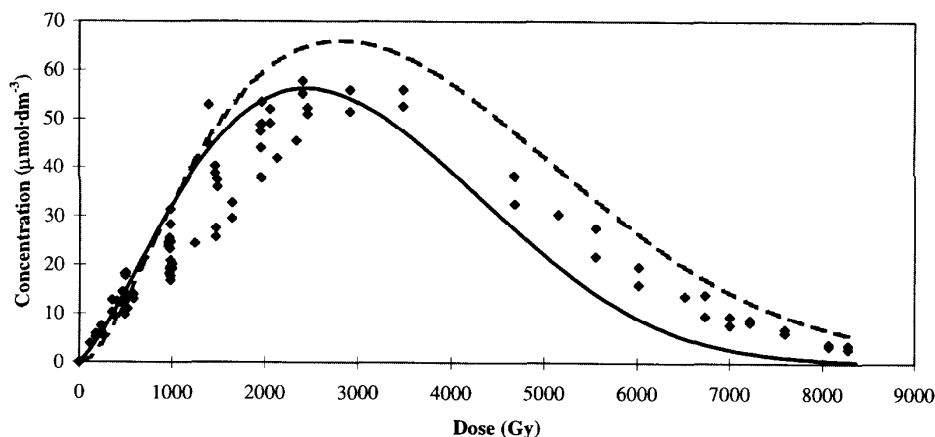
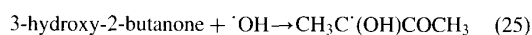


Fig. 6. Dose profile of acetaldehyde: experimental data (◆), full model prediction (—), and simplified model prediction (---).

forming an organic radical is also the rate determining step for Reaction (22), similar to the case of MEK decomposition.



Thus, the rate constant for Reaction (22), k_{1P1} , should be approximately the rate constant of Reaction (25), i.e. $k_{1P1} = 1.2 \times 10^9 \text{ dm}^3 \cdot \text{mol}^{-1} \cdot \text{s}^{-1}$ (Lilie et al., 1968).

The decomposition of 2,3-butanedione via the reaction with $\cdot\text{OH}$ is slower:



with the rate constant $1.7 \times 10^8 \text{ dm}^3 \cdot \text{mol}^{-1} \cdot \text{s}^{-1}$ (Lilie et al., 1968). This rate constant is about an order of magnitude smaller than the $\cdot\text{OH}$ reaction with 3-hydroxy-2-butanone. However, the reaction of 2,3-butanedione

with e_{aq}^- is fast with the rate constant being $1 \times 10^{10} \text{ dm}^3 \cdot \text{mol}^{-1} \cdot \text{s}^{-1}$ (Lilie et al., 1968):



Thus this reaction needs to be considered in the decomposition of 2,3-butanedione. The electron attachment on 2,3-butanedione is assumed to lead to the dissociation eventually to acetaldehyde and acetic acid, whereas the electron attachment onto organic compounds with single ketone groups does not necessarily lead to dissociation. Although there is little available experimental evidence of the decomposition of the electron attachment product, modeling results (using the full model) support the assumption (Glowa et al., 2000).

In the simplified model, the rate constants for Reac-

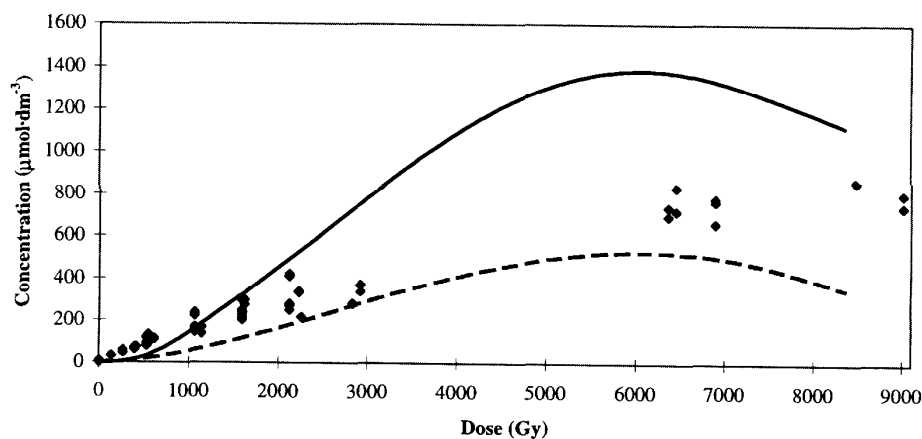


Fig. 7. Dose profile of acetic acid: experimental data (◆), full model prediction (—), and simplified model prediction (---).

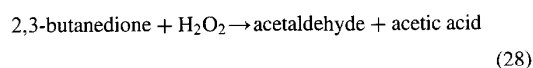
tions (23) and (24), k_{IP2-OH} and k_{IP2-E} , are assumed to be the rate constants of the initial reactions of 2,3-butanedione with $\cdot OH$ and e_{aq}^- , i.e., 1.7×10^8 and $1 \times 10^{10} \text{ dm}^3 \cdot \text{mol}^{-1} \cdot \text{s}^{-1}$, respectively. In summary, the rate constants for Reactions (22) to (24) are:

$$\begin{aligned} k_{22} (\text{s}^{-1}) &= k_{IP1} = 1.2 \times 10^9 (\text{dm}^3 \cdot \text{mol}^{-1} \cdot \text{s}^{-1}) \\ k_{23} (\text{s}^{-1}) &= k_{IP2-OH} = 1.7 \times 10^8 (\text{dm}^3 \cdot \text{mol}^{-1} \cdot \text{s}^{-1}) \\ k_{24} (\text{s}^{-1}) &= k_{IP2-E} = 1 \times 10^{10} (\text{dm}^3 \cdot \text{mol}^{-1} \cdot \text{s}^{-1}) \end{aligned}$$

It should be noted that although the rate of k_{24} is high, the contribution of the 2,3-butanedione decomposition reactions (23) and (24) to the acetic acid and acetaldehyde formation is less than that of 3-hydroxy-2-butanedione, (except at larger doses), because of the low electron concentration.

The simplified model reproduces the dose profile of 3-hydroxy-2-butanone calculated by the full model, as well as measured experimentally (Fig. 4), indicating that the kinetics of the radiolytic decomposition from 3-hydroxy-2-butanone to acetaldehyde and acetic acid can be adequately represented by one reaction step (22).

The simplified model does not reproduce the dose profile of 2,3-butanedione calculated using the full model as accurately, although the peak concentration is still reproduced within 50% of the full model results (Fig. 5). Note that for this compound, there is no experimental data to compare with. The larger discrepancy between the full and simplified model calculations for 2,3-butanedione arises due to the fact that the overall rates (rate constant \times concentration) of the initial $\cdot OH$ and e_{aq}^- reactions are relatively slow. Reactions with other radiolysis products become an important contributing factor to the decay of 2,3-butanedione. For example, the reaction with H_2O_2 contributes significantly to the decomposition of 2,3-butanedione:

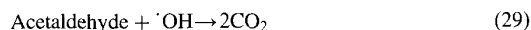


When this reaction is added, the simple model reproduce the full model result of the dose profile of 2,3-butanedione. However, its contribution to the formation of the next molecular products (acetaldehyde and acetic acid) is relatively small. As discussed above, the main route for acetaldehyde and acetic acid formation is Reaction (22). If the H_2O_2 reaction to be included in the reduced model, the behaviour of H_2O_2 also needs to be closely modelled. This reaction is not included in the simple model, which results in the differences observed between the full and reduced model calculations for acetaldehyde and acetic acid.

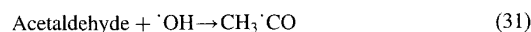
3.5. Decomposition of acetaldehyde and acetic acid to CO_2

The four carbon intermediate molecular products, 3-hydroxy-2-butanone and 2,3-butanedione decompose to two carbon molecules, acetaldehyde and acetic acid, which decompose further to CO_2 . As described earlier, assuming that the initial hydrogen abstraction reaction by $\cdot OH$ (or electron attachment followed by dissociation) is the rate determining step, the overall decay of 3-hydroxy-2-butanone (and 2,3-butanedione) to acetic acid and acetaldehyde can be simplified to Reactions (22)–(24).

Decomposition of acetaldehyde and acetic acid to the final degradation product CO_2 is also assumed to occur mainly via reactions with $\cdot OH$:

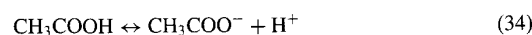


The initial hydrogen abstraction reactions, which are the rate determining steps for CO_2 production are:



where the rate constants are $1 \times 10^8 \text{ dm}^3 \cdot \text{mol}^{-1} \cdot \text{s}^{-1}$ for CH_3COO^- (acetate), $2.3 \times 10^7 \text{ dm}^3 \cdot \text{mol}^{-1} \cdot \text{s}^{-1}$ for CH_3COOH (acetic acid) and $3.6 \times 10^9 \text{ dm}^3 \cdot \text{mol}^{-1} \cdot \text{s}^{-1}$ for acetaldehyde (Buxton et al., 1988; Schuchmann and von Sonntag, 1988).

In the simplified model, the rate constant of Reaction (29) is the initial hydrogen abstraction from acetaldehyde by $\cdot OH$ (i.e., $3.6 \times 10^9 \text{ dm}^3 \cdot \text{mol}^{-1} \cdot \text{s}^{-1}$). For Reaction (30), a pH dependent rate constant (i.e., $(1 \times 10^8) \cdot (1 + K_{eq}/[H^+])$ where K_{eq} is the equilibrium constant of Reaction (34)) is used because acetate and acetic acid are in fast equilibrium [Reaction (34)].



The addition of the extra route via Reaction (33) to the simple model did not change the results, indicating that the extra reaction is not required. Because of this equilibrium, the measured concentrations of acetic acid were also the sum of acetic acid, CH_3COOH , and acetate ion, CH_3COO^- . The calculated acetic acid concentrations presented in Fig. 7 are also the sum of acetic acid and acetate ion concentrations.

The simplified model reproduces the full model results and the experimental data on the dose profile of acetaldehyde reasonably well (Fig. 6). The simplified

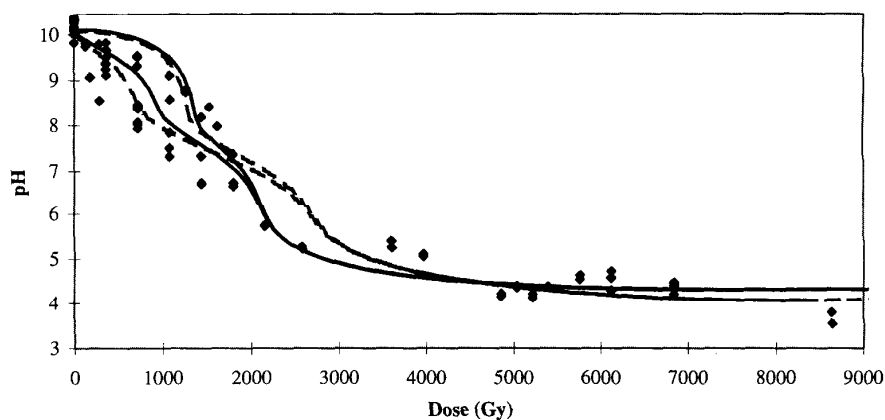


Fig. 8. Dose profile of pH: experimental data (◆), full model prediction (—), and simplified model prediction (---).

model does not reproduce the full model result on the dose profile of acetic acid/acetate, but it reproduces the experimental data better. The large discrepancy between the full and the reduced model results on acetic acid behaviour, however, has a relatively small impact on CO_2 production and pH behaviour (see Section 3.6). The reason for this is that CO_2 is produced mainly via the reaction of acetaldehyde, Reaction (29), whose rate constant is about 20 times larger than that of Reaction (30). Reaction (30) becomes important for CO_2 production only at later times or larger doses. Because CO_2 and its associated equilibria contributes significantly to the pH behaviour, the impact of the uncertainties in the overall rate of Reaction (30) on pH is also small.

3.6. pH and the concentrations of water radiolysis products

One of the key issues in determining iodine behaviour in containment is to develop the capability of predicting pH behaviour. The acid–base equilibrium of acetic acid [Equilibrium (34)] and the equilibria between CO_2 , H_2CO_3 , HCO_3^- and CO_3^{2-} must be included to properly simulate the H^+ concentration:



² Note: An inaccurate pH profile was presented in the previous report

The simplified model reproduced the observed dose profiles of pH reasonably well (Fig. 8)². The discrepancy between the full and simplified model results observed in the dose range of 2000–3000 Gy is mainly due to the difference in acetic acid concentration prediction. For the simulations (using both the full and simple models) shown in this figure, the initial total carbonated carbon concentration in the solutions was assumed to be about $2 \times 10^{-4} \text{ mol-dm}^{-3}$. This is the approximate initial carbon concentration expected in neutral pH water while in equilibrium with ordinary air. (We assume that no further CO_2 uptake takes place during the pH adjustment to 10 in the experiments.) Note that both the full and simplified model include aqueous–gas interfacial mass transfer of O_2 and CO_2 . The effect of CO_2 in the head-space of the irradiation vessel is also shown in Fig. 8. The calculated pH initially decreases quicker when gas phase CO_2 is present, than if it is not. This sensitivity to initial CO_2 concentration may account for the scatter in the pH profile of the experimental data during the first 2000 Gy.

As discussed in the introduction section, the other key parameters that need to be modelled adequately in determining iodine behaviour in containment are the steady-state concentrations of $\cdot\text{OH}$, O_2^- and H_2O_2 in the sump (Wren et al., 1999, 2000a). Fig. 9 compares the simplified model results with the full model results on the dose profiles of these water radiolysis products. The concentration of O_2^-/HO_2 in the figure is the sum of the O_2^- and HO_2 concentrations. Except during a couple of small dose ranges, the simplified model reproduces the full model results to within 50%. The discrepancy in the calculated O_2^-/HO_2 concentrations in 2000–3000 Gy is due to the difference in the pH predicted by the two models.

4. Conclusions

Methyl ethyl ketone has been studied as a model aliphatic organic compound for the radiolytic degradation of organic impurities in the sump water. Based on the experimental results and a detailed reaction kinetic model for the continuous γ -radiolysis of aerated aqueous solutions containing MEK, a simplified MEK degradation model was developed.

In the simplified model, the radiolytic decomposition of MEK in aerated aqueous solutions was approximated using single reaction steps from the reactant organic species, MEK, containing four carbon atoms to oxidized four-carbon species (3-hydroxy-2-butanone and 2,3-butanedione), from the oxidized four-carbon compounds to two-carbon species (acetaldehyde and acetic acid), and from the two-carbon intermediate products to one-carbon species (CO_2 , H_2CO_3 , HCO_3^- ,

and CO_3^{2-}). The overall rate constant for each step was approximated using the rate constant for the initial hydrogen abstraction by $\cdot\text{OH}$ from the reacting molecule. For diones, an additional path through electron attachment was required.

The simplified model, consisting of only seven reactions and four equilibria (Table 2), reproduces the experimental data and the full model results of the behaviour of MEK, the intermediate decay products and pH during the radiolysis reasonably well. The simplified model also reproduces the full model results on water radiolysis products such as H^\cdot , e_{aq}^- , $\cdot\text{OH}$, O_2^- and H_2O_2 .

The objective of the simplified organic degradation model was to calculate the values of key parameters affecting iodine behaviour in containment (pH and the concentrations of $\cdot\text{OH}$, O_2^- and H_2O_2) to match the values observed experimentally, or the values calcu-

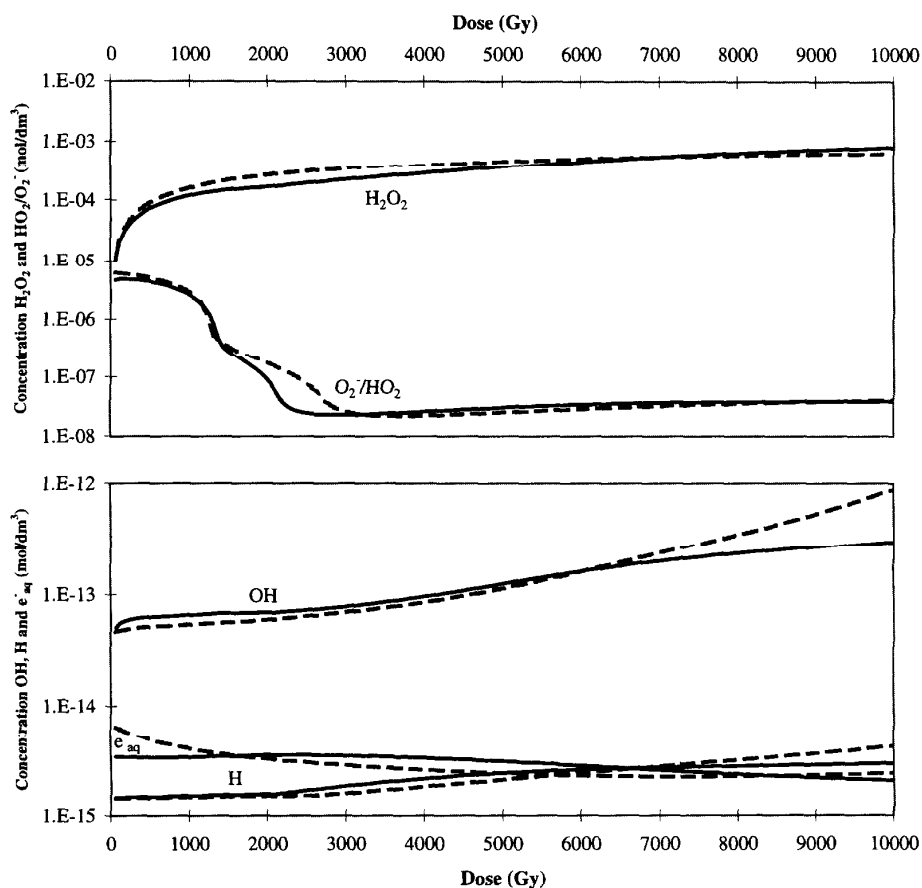


Fig. 9. Concentrations of water radiolysis products calculated by the full model (—) and simplified model (---).

lated by a comprehensive mechanistic model. An acceptable level of reproducibility should depend on the level of uncertainties that can be tolerated in the model prediction on iodine behaviour in containment. Because of various assumptions used in nuclear safety analyses, model prediction of gaseous iodine concentrations observed in large scale tests such as RTF (Radioiodine Test Facility) tests (Ball et al., 1996b; Wren et al., 1999) to within an order of magnitude is considered acceptable. This standard is partially imposed by the uncertainties in the experimental data and the uncertainties associated with postulated containment conditions. Model prediction of pH to within one unit and the concentrations of $\cdot\text{OH}$, O_2^- and H_2O_2 to within an order of magnitude must be achieved in order to meet this goal. The simplified model for MEK degradation is the first step toward obtaining a simple generic organic degradation that can be used in iodine codes. Because uncertainty in pH prediction will potentially compound when this model is applied to safety analysis, the acceptability of the simple MEK model should be more stringent. For the same reason, the simple model should also predict the intermediate degradation products whose behaviour are not required for modelling iodine behaviour. The simplified MEK model developed in this work is believed to meet these requirements.

Although this report has focused on MEK, it provides the technical basis for developing a generalized model for the radiolytic decay of other organic compounds. It may be premature to generalize the simplified reaction scheme of other organic compounds, but it may be reasonable to assume, for example, that six carbon containing organic compounds, such as methylisobutylketone (MIBK), would progress to oxidized six-carbon species, to three- and four-carbon species, to one- and two-carbon species, and eventually convert entirely to CO_2 . Measurements of MIBK concentration and pH as a function of time, without extensive measurements of intermediate products, may be sufficient to extract necessary kinetic information for MIBK. Further generalization may be possible once the relationship between the type of organic species (i.e., number of carbons, functional group, etc.), the acid production (pH drop), and the rate constant for its reaction with $\cdot\text{OH}$, is established.

Acknowledgements

The authors would like to thank Drs. C. Stuart and G. Burton at AECL for reviewing this document and for their helpful discussions. This work was funded by the COG (CANDU Owners Group) R&D Program, Working Party 06, Containment Behaviour, under the

joint participation of Ontario Power Generation, Hydro Quebec, New Brunswick Power and AECL.

References

- Ball, J.M., Hnatiw, J.B., Sims, H. 1996a. The Reduction of I_2 by H_2O_2 in Aqueous Solution. In: Güntay, S. (Ed.), Proceedings of the Fourth CSNI/OECD Workshop on the Chemistry of Iodine in Reactor Safety, Wurenlingen, Switzerland, NEA/CSNI/R(96)6, pp. 169–185.
- Ball, J.M., Kupferschmidt, W.C.H., Wren, J.C. 1996b. Results from Phase 2 of the Radioiodine Test Facility Experimental Program. In: Güntay, S. (Ed.), Proceedings of the Fourth CSNI/OECD Workshop on the Chemistry of Iodine in Reactor Safety, Wurenlingen, Switzerland, NEA/CSNI/R(96)6, pp. 63–81.
- Boyd, A.W., Carver, M.B., Dixon, R.S., 1980. Computed and experimental product concentrations in the radiolysis of water. *Radiat. Phys. Chem.* 15, 177.
- Buxton, G.V., Greenstock, C.L., Helman, W.P., Ross, A.B., 1988. Critical review of rate constants for reactions of hydrated electrons, hydrogen atoms and hydroxyl radicals ($\cdot\text{OH}/\cdot\text{O}^-$) in aqueous solution. *J. Phys. Chem. Ref. Data* 17, 513.
- Driver, P.A., Glowa, G.A., Wren, J.C., 2000. Steady-state γ -radiolysis of aqueous methyl ethyl ketone (2-butanone) under postulated nuclear reactor accident conditions. *Radiat. Phys. Chem.* 57 (1), 37–51.
- Elliot, A.J. 1994. Rate constants and G-values for the simulation of the radiolysis of light water over the range 0–300°C. Atomic Energy of Canada Limited Report, AECL-11073.
- Glowa, G.A. 1995. Phenolic compounds as potential iodine mitigants in nuclear reactor containment. MSc Thesis, University of Manitoba.
- Glowa, G.A., Driver, P.A., Wren, J.C., 2000. Irradiation of MEK part II: A detailed kinetic model for the degradation of 2-butanone in aerated aqueous solutions under steady-state γ -radiolysis conditions. *Radiat. Phys. Chem.* 58 (1) (in press).
- Lilie, J., Beck, G., Henglein, A., 1968. Pulsradiolytische Untersuchung des Acetoinradikals und des Diacetylanions in wäßriger Lösung. *Ber. Bunsenges. Phys. Chem.* 72, 579.
- Mezyk, S.P., 1994. Rate constant and activation energy determination for reaction of e^- and $\cdot\text{OH}$ with 2-butanone and propanal. *Can. J. Chem.* 72, 1116.
- Postma, A.K., Zavadoski, R.W. 1972. Review of organic iodide formation under reactor accident conditions in water-cooled reactors. Atomic Energy Commission Report, WASH-1233.
- Schuchmann, M.N., von Sonntag, C., 1988. The rapid hydration of the acetyl radical. A pulse radiolysis study of acetaldehyde in aqueous solution. *J. Am. Chem. Soc.* 110, 5698.
- Sims, H.E. 1992. A comparison of the predictions of the INSPECT code with experimental data from the AECL Whiteshell Laboratory Radioiodine Test Facility. Atomic Energy Authority, Harwell Laboratory Report, AEA-RS-2300, COG-92-332, PWR/CTG/P(92)082.

- Wren, J.C., Sagert, N.H., Sims, H.E. 1992. Modelling of Iodine Chemistry: The LIRIC Database. In: Ishigure, K., Sasaki, M., Soda, K., Sigimoto, J. (Eds.), Proceedings of the Third CSNI Workshop on Iodine Chemistry in Reactor Safety, Tokai-muri, Japan, 1991, p. 381.
- Wren, J.C., Glowa, G.A., Ball, J.M. 1996. Modelling iodine behaviour using LIRIC 3.0. In: Guntay, S. (Ed.), Proceedings of the Fourth CSNI/OECD Workshop on the Chemistry of Iodine in Reactor Safety, Wurenlingen, Switzerland, NEA/CSNI/R(96)6, pp. 507–530.
- Wren, J.C., Ball, J.M., Glowa, G.A., 1999. The interaction of iodine with organic material in containment. Nucl. Tech. 125, 337.
- Wren, J.C., Ball, J.M., Glowa, G.A., 2000a. The chemistry of iodine in containment, Nucl. Tech. 129, 297.
- Wren, J.C., Jobe, D.J., Sanipelli, G.G., Ball, J.M., 2000b. Dissolution of organic solvents from organic-based painted surfaces into water under postulated nuclear reactor accident conditions, Can. J. Chem. (in press).
- Wren, J.C., Ball, J.M., Glowa, G.A., 2000c. LIRIC, the iodine chemistry and transport model for containment under reactor accident conditions. *In preparation*.
- Zegota, H., Schuchmann, M.N., Schulz, D., von Sonntag, C., 1986. Acetylperoxy radicals, $\text{CH}_3\text{COCH}_2\text{O}_2$: A study on the γ -radiolysis and pulse radiolysis of acetone in oxygenated aqueous solutions. Z. Naturforsch. 41b, 1015.